



## Coronal Transverse Magnetohydrodynamic Waves in a Solar Prominence

T. J. Okamoto, *et al.*  
*Science* **318**, 1577 (2007);  
DOI: 10.1126/science.1145447

**The following resources related to this article are available online at  
[www.sciencemag.org](http://www.sciencemag.org) (this information is current as of December 6, 2007):**

**Updated information and services**, including high-resolution figures, can be found in the online version of this article at:

<http://www.sciencemag.org/cgi/content/full/318/5856/1577>

**Supporting Online Material** can be found at:

<http://www.sciencemag.org/cgi/content/full/318/5856/1577/DC1>

This article has been **cited by** 2 articles hosted by HighWire Press; see:

<http://www.sciencemag.org/cgi/content/full/318/5856/1577#otherarticles>

This article appears in the following **subject collections**:

Astronomy

<http://www.sciencemag.org/cgi/collection/astronomy>

Information about obtaining **reprints** of this article or about obtaining **permission to reproduce this article** in whole or in part can be found at:

<http://www.sciencemag.org/about/permissions.dtl>

that are only on the order of 0.5 km/s with a corresponding energy flux of  $\sim 0.01 \text{ W m}^{-2}$ , Tomczyk *et al.* (23) point out that line-of-sight superposition in the optically thin corona can reduce the directly observed wave amplitudes and hide the remaining wave energy flux in the large nonthermal linewidths observed with CoMP.

Once in the corona, Alfvén waves propagate quite freely, and although modelers disagree on which dissipation mechanism dominates, they agree that Alfvén waves with an energy flux of  $100 \text{ W m}^{-2}$  are vigorous enough to launch the solar wind when, inevitably, their energy is thermalized and their momentum flux is added to the wind (5, 6). Our observations of vigorous low-frequency waves obviate the need for high-frequency models in which Alfvén waves are assumed to be generated by reconnection processes in the low corona and dissipated through resonant absorption as the wave frequency becomes equal to the gyrofrequencies of the various ions in the plasma (2, 3, 24, 25). The observational support for such models has recently been challenged (26, 27). Our data, on the contrary, strongly support the recent models that are based on the dissipation of low-frequency waves; for example, because of self-interference from reflection (4, 28), compressible effects (7), or parametric decay (29, 30). Both the observed amplitudes and periods are consistent with those in comprehensive simulations that describe the generation, propagation, and dissipation of Alfvén waves from the photosphere to Earth orbit (5, 6).

#### References and Notes

1. J. W. Belcher, S. Olbert, *Astrophys. J.* **200**, 369 (1975).
2. W. I. Axford *et al.*, *Space Sci. Rev.* **87**, 25 (1999).
3. C.-Y. Tu, E. Marsch, *J. Geophys. Res.* **106**, 8233 (2001).
4. W. H. Matthaeus, G. P. Zank, S. Oughton, D. J. Mullan, P. Dmitruk, *Astrophys. J.* **523**, L93 (1999).
5. A. Verdini, M. Velli, *Astrophys. J.* **662**, 669 (2007).
6. S. R. Cranmer, A. A. van Ballegoijen, R. J. Edgar, *Astrophys. J.* **171** (suppl.), 520 (2007).
7. T. K. Suzuki, S.-i. Inutsuka, *J. Geophys. Res.* **111**, A06101 (2006).
8. S. Tsuneta *et al.*, *Sol. Phys.*, <http://arxiv.org/abs/0711.1715>.
9. T. Kosugi, *et al.*, *Sol. Phys.* **243**, 3 (2007).
10. B. De Pontieu *et al.*, *Publ. Astron. Soc. Jpn.* **59**, S655 (2007).
11. For a discussion on MHD kink-mode waves, see the supporting online material (SOM).
12. Methods are available as supporting material on *Science Online*.
13. For a discussion on what may determine the periods, see the SOM.
14. V. H. Hansteen, B. Gudiksen, *ESA Spec. Pub.* **592**, 87 (2005).
15. V. H. Hansteen, M. Carlsson, B. Gudiksen, *Astron. Soc. Pac. Conf. Ser.* **368**, 107 (2007).
16. T. Kudoh, K. Shibata, *Astrophys. J.* **514**, 493 (1999).
17. J. V. Hollweg, *Sol. Phys.* **56**, 305 (1978).
18. J. V. Hollweg, *Sol. Phys.* **70**, 25 (1981).
19. J. V. Hollweg, S. Jackson, D. Galloway, *Sol. Phys.* **75**, 35 (1982).
20. J. M. Beckers, *Sol. Phys.* **3**, 367 (1968).
21. J. Trujillo Bueno, L. Merenda, R. Centeno, M. Collados, E. Landi Degl'Innocenti, *Astrophys. J.* **619**, L191 (2005).
22. V. H. Hansteen, E. Leer, *J. Geophys. Res.* **100**, 21577 (1995).
23. S. Tomczyk *et al.*, *Science* **317**, 1192 (2007).
24. S. R. Cranmer, G. B. Field, J. L. Kohl, *Astrophys. J.* **518**, 937 (1999).
25. S. R. Cranmer *et al.*, *Astrophys. J.* **511**, 481 (1999).
26. N.-E. Raouafi, S. K. Solanki, *Astron. Astrophys.* **412**, 271 (2003).
27. N.-E. Raouafi, J. W. Harvey, S. K. Solanki, *Astrophys. J.* **658**, 643 (2007).
28. M. Velli, *Astron. Astrophys.* **270**, 304 (1993).
29. F. Pruneti, M. Velli, *ESA Spec. Pub.* **404**, 623 (1997).
30. L. Del Zanna, M. Velli, P. Londrillo, *Astron. Astrophys.* **367**, 705 (2001).
31. This research was supported by NASA grants NNG06GG79G, NNG06GC89G, and NM07AA01C (Hinode/SOT); NSF grant ATM-0541567; and the Research Council of Norway through grant 170935/V30 and through grants of computing time from the Programme for Supercomputing. B.D.P. thanks the Institute of Theoretical Astrophysics/Oslo group and S.W.M. for excellent hospitality. We thank the Hinode/SOT team for building an excellent instrument. Hinode is a Japanese mission developed and launched by the Institute of Space and Astronautical Science/Japan Aerospace Exploration Agency (ISAS/JAXA), with the National Astronomical Observatory of Japan (NAO) as domestic partner and NASA and the Science and Technology Facilities Council (UK) as international partners. It is operated by these agencies in cooperation with the European Space Agency and Norwegian Space Centre (Norway). The SOT was developed jointly by NAO, the Lockheed Martin Solar and Astrophysics Laboratory, ISAS/JAXA, NASA, the High Altitude Observatory, and Mitsubishi Electric Corporation.

#### Supporting Online Material

[www.sciencemag.org/cgi/content/full/318/5856/1574/DC1](http://www.sciencemag.org/cgi/content/full/318/5856/1574/DC1)  
Materials and Methods

SOM Text

Figs. S1 to S6

References

Movies S1 to S5

22 May 2007; accepted 13 November 2007  
10.1126/science.1151747

#### REPORT

## Coronal Transverse Magnetohydrodynamic Waves in a Solar Prominence

T. J. Okamoto,<sup>1,2\*</sup> S. Tsuneta,<sup>1</sup> T. E. Berger,<sup>3</sup> K. Ichimoto,<sup>1</sup> Y. Katsukawa,<sup>1</sup> B. W. Lites,<sup>4</sup> S. Nagata,<sup>2</sup> K. Shibata,<sup>2</sup> T. Shimizu,<sup>5</sup> R. A. Shine,<sup>3</sup> Y. Suematsu,<sup>1</sup> T. D. Tarbell,<sup>3</sup> A. M. Title<sup>3</sup>

Solar prominences are cool  $10^4$  kelvin plasma clouds supported in the surrounding  $10^6$  kelvin coronal plasma by as-yet-undetermined mechanisms. Observations from Hinode show fine-scale threadlike structures oscillating in the plane of the sky with periods of several minutes. We suggest that these represent Alfvén waves propagating on coronal magnetic field lines and that these may play a role in heating the corona.

Solar prominences are classified as either quiescent or active region (AR), the latter referring to material suspended above sunspot magnetic regions. Quiescent prominences often exist for many weeks at high solar latitudes, whereas AR prominences can be dynamic and short-lived. They are the most enigmatic of solar structures supported by coronal magnetic field lines, sometimes erupting as the source of coronal mass ejections, large-scale eruptions of plasma from flaring solar active regions, that can have major impacts on the terrestrial magnetic environment. Recent ground-based observations have revealed

that AR prominences have numerous small threadlike features (1), with continuous flow of material along the threads (2–9). Observations from space (10, 11) confirm these findings and show additional dynamics related to coronal structure.

We report Hinode Solar Optical Telescope (SOT) (12, 13) observations of an AR prominence in a 0.3-nm broadband region centered at 396.8 nm, the H-line spectral feature of singly ionized calcium (Ca II). Radiation in this bandpass typically has a temperature of less than 20,000 K.

We obtained over 1 hour of continuous SOT images of NOAA AR 10921 on the west solar

limb on 9 November 2006. The images show a multithreaded AR prominence suspended above the main sunspot (Fig. 1). Although no simultaneous  $H\alpha$  images were taken, the Ca II H-line prominence structures are consistent with the structures seen in lower-resolution  $H\alpha$  observations (14). The Ca II H-line movie (movie S1) shows ubiquitous continuous horizontal motions along the prominence threads. The origins of these flows remain unknown. Some of the flows had constant speeds of about  $40 \text{ km s}^{-1}$ , whereas others accelerated monotonically in a more complicated fashion.

The Hinode SOT movies also reveal that many of the threads in the prominence underwent vertical (i.e., in the plane of the sky) oscillatory motions (Fig. 2) at periods of 130 to 250 s. The

<sup>1</sup>National Astronomical Observatory (NAO), Mitaka, Tokyo 181-8588, Japan. <sup>2</sup>Kwasan and Hida Observatories, Kyoto University, Yamashina, Kyoto 607-8471, Japan. <sup>3</sup>Lockheed Martin Solar and Astrophysics Laboratory, B/252, 3251 Hanover Street, Palo Alto, CA 94304, USA. <sup>4</sup>High Altitude Observatory, National Center for Atmospheric Research, Post Office Box 3000, Boulder CO 80307–3000, USA. <sup>5</sup>Institute of Space and Astronautical Science, Japan Aerospace Exploration Agency (ISAS/JAXA), Sagamihara, Kanagawa 229-8510, Japan.

\*To whom correspondence should be addressed. E-mail: [joten.okamoto@nao.ac.jp](mailto:joten.okamoto@nao.ac.jp)

# Hinode

vertical oscillatory motions were coherent over lengths as long as 16,000 km. One thread (Fig. 3A) had a vertical width of 660 km and an oscillation period of 240 s. Comparison of the oscillation phase at various horizontal positions (Fig. 3, B to F) reveals that the thread oscillated in phase along its entire length. The vertical oscillation amplitudes of all threads we saw ranged from 400 to 1800 km, and thread widths were between 430 and 660 km (Table 1). Because we cannot determine the angle between the plane of oscillation and the line of sight to the prominence threads, the oscillation amplitudes as well as the horizontal velocities are minimum estimates.

The observed vertical oscillatory motion is most likely due to propagating or standing Alfvén waves on the horizontal magnetic field lines that compose the prominence. An alternate hypothesis is longitudinal plasma motion along helical field lines. Helical field line structure has been observed in many previous prominence studies (15–17); however, the helical field line hypothesis cannot explain the several cases we found of synchronous vertical oscillation of entire threads, for example, Fig. 3. Alternately, if the observed threads are thin magnetic flux tubes, the observed oscillations may be fast magneto-acoustic kink modes propagating along the tubes (18, 19). The observations shown here lack line-of-sight Doppler velocity measurements, so we cannot determine the exact oscillation mode at this point.

These field lines connect to the source regions in the photosphere (7), where they are excited by the wide-spectrum p-mode oscillations originating in the convection zone. Each field line oscillated independently, as seen in the Hinode movies. The synchronous oscillation along entire threads shown in Fig. 3 implies that we cannot distinguish the time difference at the minimum and maximum amplitudes all along the thread. The uncertainty in phase of the oscillation is no more than 1/16 of the oscillation period, so we

estimate that the minimum wavelength of the oscillation is  $16 \times 16,000 \approx 250,000$  km. The wave speed is estimated to be  $>1050 \text{ km s}^{-1}$  for the average oscillation period of  $\sim 240$  s. If we assume that the plasma density is  $10^{10} \text{ cm}^{-3}$  (20),

the implied magnetic field strength is  $\sim 50$  G for the propagating Alfvén wave, in agreement with measurements and models of active region prominence magnetic fields (21, 22). The Poynting flux carried by the observed waves is then estimated

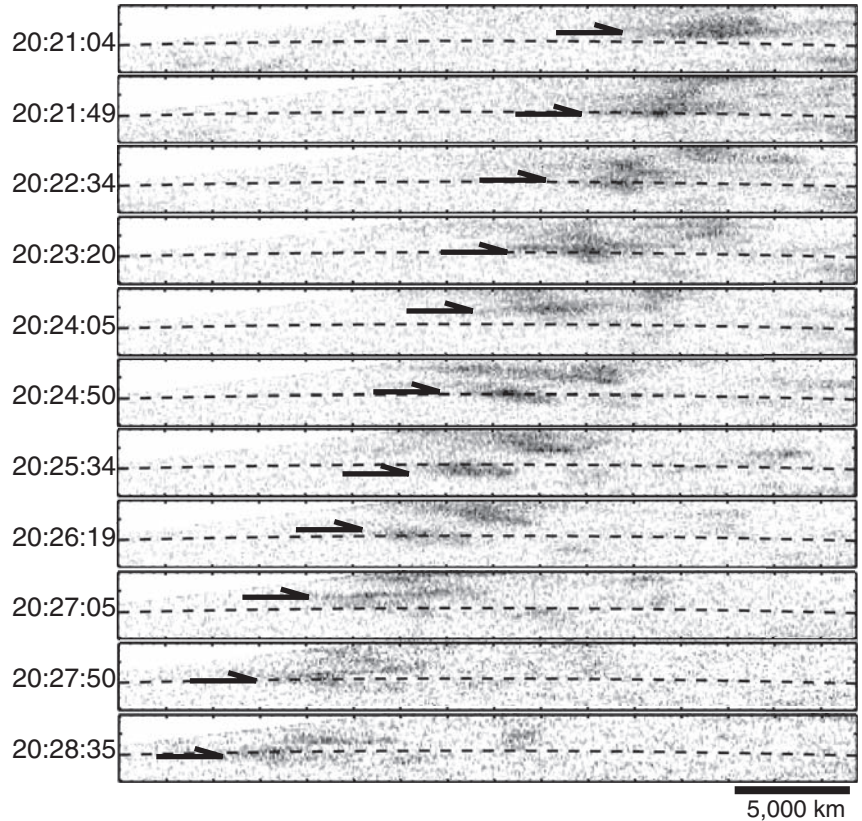
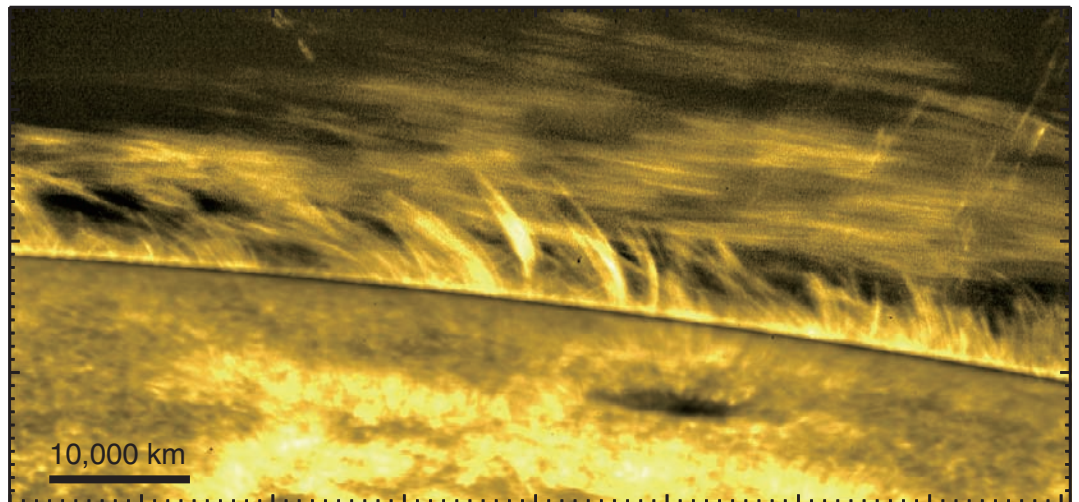


**Fig. 2.** Example of a vertical oscillation of a single prominence thread. A small field of view is extracted from the larger field shown in Fig. 1 and shown in negative contrast. Tick marks have a spacing of 2000 km on the Sun, and UT time for each image is denoted on the left. The dashed line in each image indicates an approximately constant height above the photosphere. This oscillating thread has a length of about 3600 km and width of 430 km. Steady flow at  $39 \text{ km s}^{-1}$  along the thread is evident. The vertical amplitude of the oscillation is about 900 km with a period of 174 s. The vertical speed is about  $10 \text{ km s}^{-1}$ .

**Fig. 1.** High-resolution image on the solar limb obtained with SOT aboard Hinode. This observation was performed with a cadence of 15 s from 19:33 to 20:44 UT on 9 November 2006. Tick marks have a spacing of 1000 km on the Sun. A radial density filter is applied to show the brighter photosphere and the fainter coronal structures in the same image. The main sunspot of NOAA AR 10921 as well as the trailing bright plage areas are visible on the disk. Above the limb, ubiquitous vertical spicules are seen below the horizontal threads of the AR prominence. The cloudlike prominence structure is located 10,000 to 20,000 km above the visible limb and exhibits a very complex fine structure with predominant horizontal threadlike features. The intensity of the prominence in Ca II H-line radiation is about 1% of the on-disk photosphere.



to be  $\rho v^2 V_A \sim 2.0 \times 10^6 \text{ erg s}^{-1} \text{ cm}^{-2}$  (where  $\rho$  is the density,  $v$  is the velocity amplitude, and  $V_A$  is the Alfvén speed), a lower limit based on the minimum estimates of observed tangential velocities. Given a suitable dissipation mechanism, this flux is sufficient to heat coronal loops with lengths longer than the estimated oscillation wavelength (23).

In transiting from the photosphere to the chromosphere, the large density decrease with height results in rapid increases in the acoustic and Alfvén wave propagation speeds. This effective dis-

continuity causes waves with periods longer than a cutoff period determined by the thermodynamic conditions and magnetic field strength in the atmosphere to be reflected before reaching the coronal heights of active region prominences. Because we find a typical oscillation period  $\sim 240$  to 250 s, we can infer that the Alfvén cutoff period is longer than about 4 min for this prominence structure.

The limited field of view of our data prevents us from determining the lengths of the field lines threading the prominence. However, the frequency spectrum of the observed waves can be used to

investigate the length of the field lines. Open field lines have a distinct wide spectrum above the Alfvén cutoff frequency, whereas shorter closed loops show multiple discrete resonances as a function of loop length. The estimated Alfvén speed and the mean observed period implies a minimum length of 250,000 km if this is the standing wave in a closed-loop system.

Previous observations of waves in the solar corona include Doppler velocity and periodic intensity oscillations in coronal loops as well as flare-generated transversal displacements of active region loops (24–28). Those oscillations are examples of magneto-acoustic waves propagating out from photospheric source sites. Alfvén waves in coronal loops and prominences are also claimed to account for spectroscopic observations of nonthermal line widths in coronal emission lines (29, 30).

**Table 1.** Properties of moving threads with vertical oscillations. Asterisks mean averaged velocity.

	Length (km)	Width (km)	Horizontal velocity ( $\text{km s}^{-1}$ )	Vertical oscillation period (s)	Vertical oscillation width (km)	Height from the limb (km)
1	3600	430	39	$174 \pm 25$	904	18,300
2	16,000	660	15	$240 \pm 30$	1113	12,400
3	6700	580	39	$230 \pm 87$	909	14,700
4	2200	360	46*	$180 \pm 137$	435	19,000
5	3500	430	45*	$135 \pm 21$	408	14,300
6	1700	510	25*	$250 \pm 17$	1771	17,200

**References and Notes**

1. Y. Lin, O. Engvold, L. Rouppe van der Voort, J. E. Wiik, T. E. Berger, *Sol. Phys.* **226**, 239 (2005).
2. J. C. Vial, P. Gouttebroze, G. Artzner, P. Lemaire, *Sol. Phys.* **61**, 39 (1979).

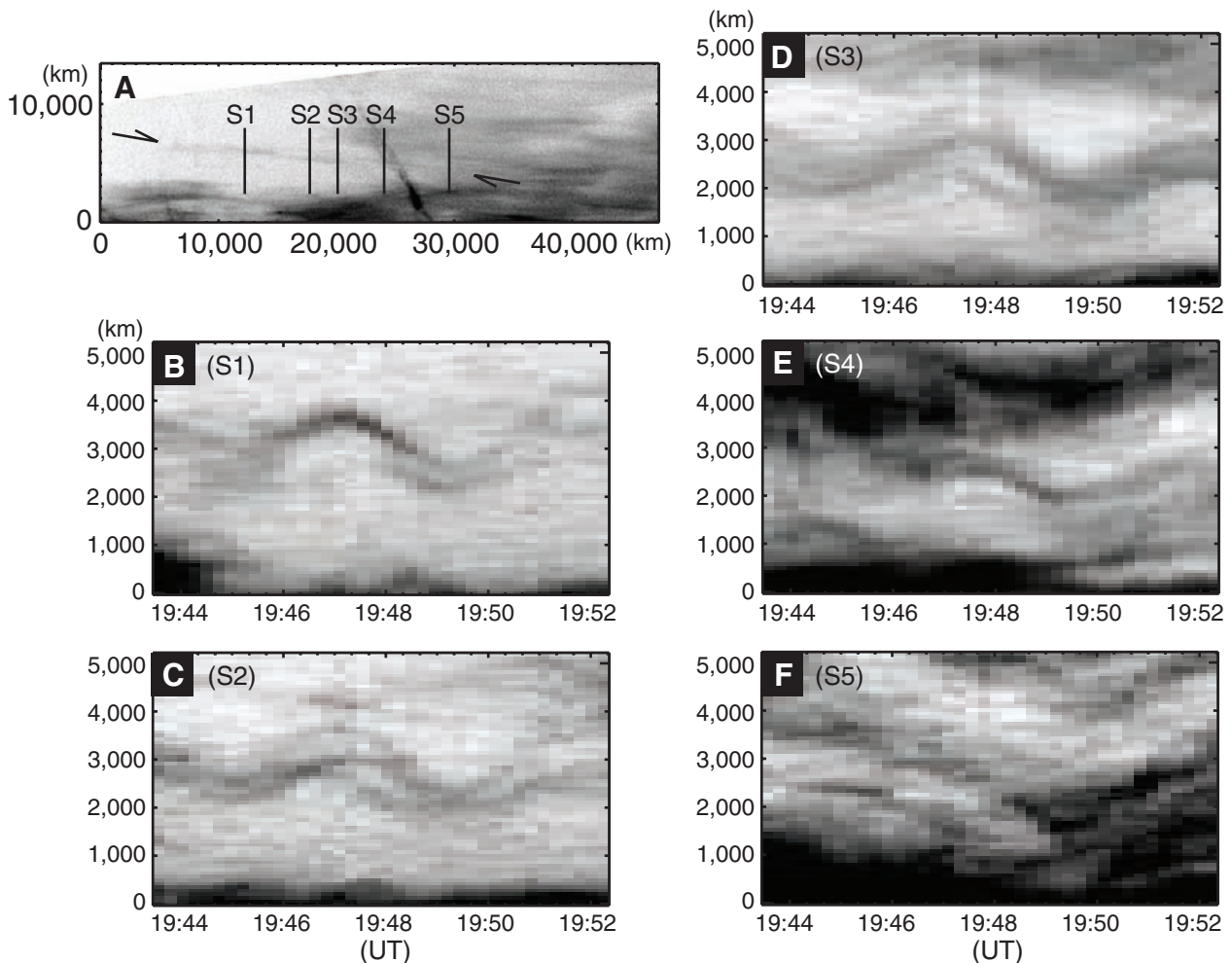


**Fig. 3.** Example of a prominence thread undergoing synchronous oscillation along its entire length. (A) The long thread extending  $\sim 16,000$  km. Lines S1 to S5 indicate the locations of height versus time plots shown in (B to F). The arrows indicate both

sides of the long thread oscillating synchronously. (B to F) Height-time plots (shown in negative contrast) for the locations indicated in (A). Maximum and minimum amplitudes occur at nearly the same time for all locations.

3. J. M. Malherbe, B. Schmieder, E. Ribes, P. Mein, *Astron. Astrophys.* **119**, 197 (1983).
4. G. Simon, B. Schmieder, P. Démoulin, A. I. Poland, *Astron. Astrophys.* **166**, 319 (1986).
5. B. Schmieder, M. A. Raadu, J. E. Wiik, *Astron. Astrophys.* **252**, 353 (1991).
6. S. F. Martin, *Sol. Phys.* **182**, 107 (1998).
7. J. B. Zirker, O. Engvold, S. F. Martin, *Nature* **396**, 440 (1998).
8. J. Chae, C. Denker, T. J. Spirock, H. Wang, P. R. Goode, *Sol. Phys.* **195**, 333 (2000).
9. J. T. Karpen, S. K. Antiochos, J. A. Klimchuk, *Astrophys. J.* **637**, 531 (2006).
10. C. J. Schrijver *et al.*, *Sol. Phys.* **187**, 261 (1999).
11. S. Patsourakos, J. C. Vial, *Sol. Phys.* **208**, 253 (2002).
12. T. Kosugi *et al.*, *Sol. Phys.* **243**, 3 (2007).
13. S. Tsuneta *et al.*, <http://arxiv.org/abs/0711.1715>.
14. Y. Suematsu, R. Yoshinaga, N. Terao, T. Tsubaki, *Publ. Astron. Soc. Jpn.* **42**, 187 (1990).
15. M. Kuperus, M. A. Raadu, *Astron. Astrophys.* **31**, 189 (1974).
16. J. L. Leroy, V. Bommier, S. Sahal-Bréchet, *Astron. Astrophys.* **131**, 33 (1984).
17. T. Hirayama, *Sol. Phys.* **100**, 415 (1985).
18. V. M. Nakariakov, E. Verwichte, *Living Rev. Sol. Phys.* **2**, 3 (2005).
19. A. J. Díaz, R. Oliver, J. L. Ballester, *Astrophys. J.* **580**, 550 (2002).
20. T. Hirayama, in *Coronal and Prominence Plasma*, A. I. Poland, Ed., NASA Conference Publication No. 2442 (NASA, Washington, DC, 1986).
21. E. Tandberg-Hanssen, J. M. Malville, *Sol. Phys.* **39**, 107 (1974).
22. E. Wiehr, G. Stellmacher, *Astron. Astrophys.* **247**, 379 (1991).
23. G. L. Withbroe, R. W. Noyes, *Annu. Rev. Astron. Astrophys.* **15**, 363 (1977).
24. I. De Moortel, J. Ireland, A. W. Hood, R. W. Walsh, *Astron. Astrophys.* **387**, L13 (2002).
25. C. J. Schrijver, M. J. Aschwanden, A. M. Title, *Sol. Phys.* **206**, 69 (2002).
26. M. J. Aschwanden, B. De Pontieu, C. J. Schrijver, A. M. Title, *Sol. Phys.* **206**, 99 (2002).
27. D. Banerjee, R. Erdélyi, R. Oliver, E. O'Shea, *Sol. Phys. tmp*, 136 (2007).
28. Y. Lin, O. Engvold, L. H. M. Rouppe van der Voort, M. van Noort, *Sol. Phys. tmp*, 71 (2007).
29. S. Koutchmy, Y. D. Zuzgda, V. Locans, *Astron. Astrophys.* **120**, 185 (1983).
30. H. Hara, K. Ichimoto, *Astrophys. J.* **513**, 969 (1999).
31. The authors thank H. Shibahashi, T. Sekii, R. Erdélyi, and V. Nakariakov for comments. Hinode is a Japanese mission developed and launched by ISAS/JAXA, with NAOJ as domestic partner and NASA and Science and Technology Facilities Council (STFC) (UK) as international partners. It is operated by these agencies in cooperation with European Space Agency and Norwegian Space Centre (Norway). This work was carried out at the NAOJ Hinode science center, which was supported by the Grant-in-Aid for Creative Scientific Research, the Basic Study of Space Weather Prediction (head investigator, K.S.) from the Ministry of Education, Culture, Sports, Science, and Technology, Japan, donation from Sun Microsystems Incorporated, and NAOJ internal funding. The National Center for Atmospheric Research is sponsored by NSF. T.J.O. is supported by research fellowships from the Japan Society for the Promotion of Science for Young Scientists.

**Supporting Online Material**

[www.sciencemag.org/cgi/content/full/318/5856/1577/DC1](http://www.sciencemag.org/cgi/content/full/318/5856/1577/DC1)  
Movie S1

21 May 2007; accepted 6 November 2007  
10.1126/science.1145447

REPORT

# Evidence for Alfvén Waves in Solar X-ray Jets

J. W. Cirtain,<sup>1,2\*</sup> L. Golub,<sup>1</sup> L. Lundquist,<sup>1</sup> A. van Ballegooijen,<sup>1</sup> A. Savcheva,<sup>1</sup> M. Shimojo,<sup>3</sup> E. DeLuca,<sup>1</sup> S. Tsuneta,<sup>4</sup> T. Sakao,<sup>5</sup> K. Reeves,<sup>5</sup> M. Weber,<sup>1</sup> R. Kano,<sup>4</sup> N. Narukage,<sup>5</sup> K. Shibasaki<sup>3</sup>

Coronal magnetic fields are dynamic, and field lines may misalign, reassemble, and release energy by means of magnetic reconnection. Giant releases may generate solar flares and coronal mass ejections and, on a smaller scale, produce x-ray jets. Hinode observations of polar coronal holes reveal that x-ray jets have two distinct velocities: one near the Alfvén speed (~800 kilometers per second) and another near the sound speed (200 kilometers per second). Many more jets were seen than have been reported previously; we detected an average of 10 events per hour up to these speeds, whereas previous observations documented only a handful per day with lower average speeds of 200 kilometers per second. The x-ray jets are about  $2 \times 10^3$  to  $2 \times 10^4$  kilometers wide and  $1 \times 10^5$  kilometers long and last from 100 to 2500 seconds. The large number of events, coupled with the high velocities of the apparent outflows, indicates that the jets may contribute to the high-speed solar wind.

The solar corona provides an opportunity to study the interactions of high-temperature electrically conducting gas, plasma, and a dynamic magnetic field. The constant emergence and cancellation of the magnetic field create a multitude of energetic changes in magnetic topology that can inject enormous amounts of energy into the plasma. It is thought that magnetic reconnection is involved in releasing energy to produce solar flares and coronal mass ejections (CMEs). X-ray jets, in which a burst of hot plasma is driven into the solar corona along an open magnetic field line, are thought to be a different manifestation of the reconnection process. It appears as though at least some fraction of these outflows has sufficient kinetic energy to leave the corona and propagate into the inner heliosphere.

Two types of outflows are possible during the post-magnetic reconnection phase of a jet. In the first case, an outflow at the local sound speed ( $v_c$ ), resulting from energy deposition that rapidly heats the dense chromospheric plasma, expands into the overlying low-pressure corona. The sound speed is governed by the equation

$$v_c = \left( \frac{2\gamma kT^{1/2}}{m_p} \right)^{1/2} \quad (1)$$

Here,  $T$  is the temperature at the location of energy deposition,  $k$  is the Boltzmann constant,  $\gamma$  is the ratio of specific heat capacities, and  $m_p$  is the proton mass. The average temperature of jets and the related footpoint flares is 6 million K ( $1, 2$ ), a temperature estimate consistent with our observations, which also show that the loop density in the coronal hole

before the jet is  $3 \times 10^8 \text{ cm}^{-3}$ . The initial velocity of the conduction front would be  $400 \text{ km s}^{-1}$ .

The second case is when plasma is accelerated by the formation of an Alfvén wave during the relaxation of the magnetic field, and the plasma is forced to flow out along the field at about the Alfvén speed,  $v_a$ , given by

$$v_a = B_0 / \sqrt{4\pi\rho} \quad (2)$$

where  $B_0$  is the magnetic field strength, and  $\rho$  is the mass density. Assuming that the magnetic field is of the order of 10 gauss, the Alfvén velocity of the plasma before the subsequent evaporation should be  $\sim 1000 \text{ km s}^{-1}$ .

These observations of coronal jets provide useful insight into the formation of hot, collimated, high-velocity outflows, which are likely a large-scale contributor to the mass loading of the fast solar wind. The first models for the existence of the solar wind were provided by Parker and Chapman (3, 4). Previous work (5–9) has suggested that Alfvén waves may play an important role in driving the solar wind. Using observations from the NASA mission Ulysses, Wang (10) found that the fast solar wind originated from the polar coronal holes and was nearly continuously present, but there was no direct evidence for the mechanism producing the fast wind.

<sup>1</sup>Harvard-Smithsonian Center for Astrophysics, 60 Garden Street, Cambridge, MA 02138, USA. <sup>2</sup>Marshall Space Flight Center, National Aeronautics and Space Administration (NASA) VP62, Huntsville, AL 35812, USA. <sup>3</sup>Nobeyama Solar Radio Observatory, Nobeyama, Nagano 384–1305, Japan. <sup>4</sup>National Astronomical Observatory of Japan (NAOJ), Mitaka, Tokyo 181–8588, Japan. <sup>5</sup>Institute of Space and Astronautical Science, (ISAS), Japan Aerospace Exploration Agency (JAXA), Sagamihara, Kanagawa 229–8510, Japan.

\*To whom correspondence should be addressed. E-mail: Jonathan.W.Cirtain@nasa.gov